

## Photoinduced demagnetization and its dynamical behavior in a $(\text{Nd}_{0.5}\text{Sm}_{0.5})_{0.6}\text{Sr}_{0.4}\text{MnO}_3$ thin film

K. Matsuda,\* A. Machida, Y. Moritomo, and A. Nakamura

*Department of Applied Physics, Faculty of Engineering, and Center for Integrated Research in Science and Engineering (CIRSE), Nagoya University, Chikusa-ku, Nagoya, 464-8603 Japan*

(Received 30 March 1998)

We have observed a significant change of absorption spectrum in the visible region by the irradiation of an intense laser pulse in a double-exchange ferromagnet  $(\text{Nd}_{0.5}\text{Sm}_{0.5})_{1-x}\text{Sr}_x\text{MnO}_3$  ( $x=0.4$ ) thin film. In the ferromagnetic state, the increase of spectral weight of the interband transition between  $J$ -split bands has been observed, indicating that the photoexcited  $e_g$  carriers suppress the neighboring spin correlation. The time-resolved spectroscopy in a vast time domain from 100 fs to 1  $\mu\text{s}$  has shown that the photoinduced demagnetization occurs within 200 ps after the photoinjection and spin correlation recovers in 300 ns. We further found that the demagnetization efficiency strongly depends on the spin direction of the excited  $e_g$  carriers. [S0163-1829(98)52332-6]

Recently, there has been increasing interest in photoinduced magnetization and magnetic transition in various magnetic materials. In a diluted magnetic semiconductor heterostructure of  $\text{In}_{0.94}\text{Mn}_{0.06}\text{As}/\text{GaSb}$ ,<sup>1</sup> the cw light irradiation at low temperature induces a permanent ferromagnetic order via spin-exchange interactions between photoinjected holes and Mn spins. The magnetization buildup by a circularly polarized light has been observed for a  $\text{CdTe}/\text{Cd}_{1-x}\text{Mn}_x\text{Te}$  multiple-quantum-well structure in the absence of seeding magnetic field.<sup>2</sup> In a Prussian blue analogue  $\text{K}_{0.2}\text{Co}_{1.4}[\text{Fe}(\text{CN})_6]\cdot 6.9\text{H}_2\text{O}$ , the ferrimagnetic transition temperature  $T_c$  is increased by irradiation of cw light from 16 to 19 K.<sup>3</sup>

Other candidate materials that show a photoinduced effect are doped manganites, in which the ferromagnetic interaction is mediated by the itinerant  $e_g$  carriers (double-exchange interaction<sup>4</sup>). In this system, the photoexcited  $e_g$  carriers are expected to significantly affect the magnetic interaction, and to modify the  $t_{2g}$ -spin ordering. The doped manganites have a characteristic electronic structure, reflecting the strong on-site exchange interaction ( $J \sim 3$  eV).<sup>5</sup> As the one-electron bandwidth  $W$  of the  $e_g$  state is much smaller than the  $J$  value, the  $e_g$  band is split into two bands ( $J$ -split bands).<sup>5-8</sup> Actually, we found a characteristic absorption band at  $\sim 3$  eV due to the interband transition between the  $J$ -split bands (see the inset of Fig. 1); the spectral weight decreases with magnetization  $M$  as  $\propto [1 - (M/M_s)^2]$ , where  $M_s$  is the saturation magnetization.<sup>5</sup> Thus, the interband transition is a sensitive monitor of the nearest-neighbor spin correlation  $\langle S_i S_{i+1} \rangle$ , or macroscopic magnetization.

In this paper, we report on a significant change in spin alignment by the photoinjection of  $e_g$  carriers and its dynamical aspect in a doped manganite thin film  $(\text{Nd}_{0.5}\text{Sm}_{0.5})_{1-x}\text{Sr}_x\text{MnO}_3$  ( $x=0.4$ ). In the ferromagnetic phase, we observed an increase in absorption due to the interband transition by the irradiation of a femtosecond or nanosecond laser pulse, indicating a decrease of magnetization in the  $t_{2g}$ -localized spin. The demagnetization efficiency depends strongly on the spin direction of the excited  $e_g$  carriers; down-spin  $e_g$  electrons antiparallel to the  $t_{2g}$  spin more

effectively induce the demagnetization, being of the order of  $\sim 0.1M_s$  for the excitation photon density of  $\sim 8 \times 10^{19} \text{ cm}^{-3}$ . The photoinduced demagnetization occurs in 200 ps after the pump-pulse excitation and the ferromagnetic ground state recovers in 300 ns.

The samples used in this study were  $(\text{Nd}_{0.5}\text{Sm}_{0.5})_{1-x}\text{Sr}_x\text{MnO}_3$  ( $x=0.4$ ) thin films with a thickness of  $\sim 200$  nm grown on  $\text{MgO}$  (100) substrates. The growth condition by the laser ablation has been reported in our previous paper.<sup>5</sup> Temperature dependence of magnetization was measured in a field of 0.5 T after cooling down to 5 K in zero field, and the result shows that the ferromagnetic phase transition temperature  $T_c$  in the sample studied here is approximately 155 K. The transient absorption spectra in the time domain of 100 fs–1 ns were measured by means of a pump-probe method with a  $\text{Ti}:\text{Al}_2\text{O}_3$  regenerative amplifier laser system. The pulse duration, photon energy, and fluence of the pump pulse were 100 fs, 3.20 eV, and 0.2  $\text{mJ}/\text{cm}^2$ , respectively. Details of the measurement systems of the femtosecond pump-probe experiment have been described in Ref. 9. The pump and probe experiments in the time domain between ns and  $\mu\text{s}$  were performed using an excimer laser pumped dye laser with a pulse duration of 20 ns as a pump pulse and a high-pressure Xe flash lamp as a probe pulse. The tuning wavelength range of the dye laser was 332–875 nm. The temporal behavior on the time scale of several tens of nanoseconds was measured using a boxcar integrator.

Before describing details of experimental results, let us explain the electronic structure seen in the absorption spectrum of doped manganites. The inset of Fig. 1(a) shows the absorption spectra  $\alpha(\omega)$  for  $(\text{Nd}_{0.5}\text{Sm}_{0.5})_{0.6}\text{Sr}_{0.4}\text{MnO}_3$  above and below  $T_c$  ( $=155$  K). The temperature-independent component (hatched region in the inset) has been ascribed to the charge-transfer (CT) type excitation from oxygen  $2p$  to Mn  $3d$  bands.<sup>5,6</sup> The lower- ( $\sim 1.2$  eV) and higher-lying ( $\sim 4.4$  eV) peak structures correspond to the up-spin  $[t_{2g}^3(\uparrow)e_g(\uparrow)\underline{L}]$  and down-spin  $[t_{2g}^3(\downarrow)e_g(\downarrow)\underline{L}]$  excitations, respectively. The temperature-sensitive components observed in 2.2–4.0 eV and below 1.3 eV are due to the interband transition between the  $J$ -split bands and intraband transition within the lower band, respectively.<sup>5</sup> Hereafter, we

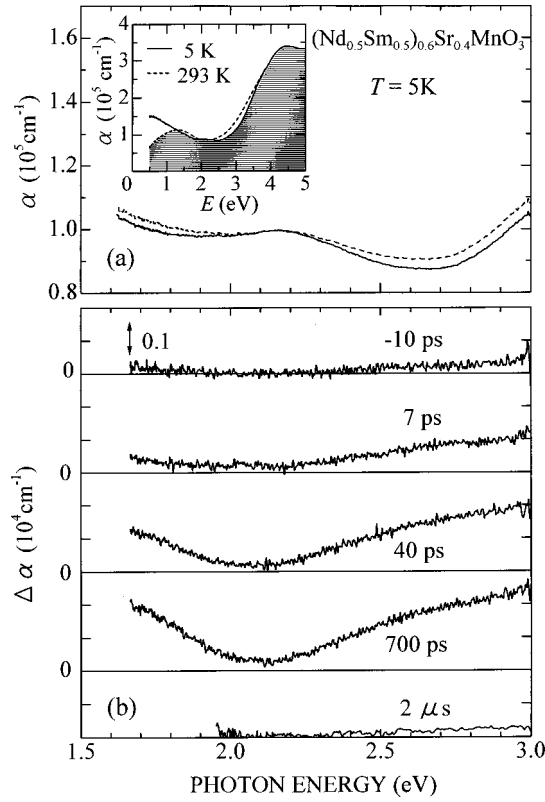


FIG. 1. (a) Absorption spectra for the  $(\text{Nd}_{0.5}\text{Sm}_{0.5})_{0.6}\text{Sr}_{0.4}\text{MnO}_3$  thin film before (solid curve) and after pump-pulse excitations (dashed curve). Inset shows the absorption spectra at 5 and 293 K. The hatched region represents the temperature-independent charge-transfer (CT) component. (b) Differential absorption spectra  $\Delta\alpha(\omega)$  in ferromagnetic phase at 5 K. The excitation photon energy and density are 3.20 eV and  $\sim 8 \times 10^{19} \text{ cm}^{-3}$ , respectively. Delay times between pump and probe pulses are shown in the figure.

refer to the former transition as a  $J$ -gap transition. Shown in Fig. 1(b) are the differential absorption spectra at 5 K in the ferromagnetic phase after the pump-pulse excitation with the photon energy of 3.20 eV. The differential absorption spectrum  $\Delta\alpha$  is defined as the difference between pumped and unpumped spectra. The positive  $\Delta\alpha$ , that is, induced absorption, is observed for 2.2–3.0 eV and 1.65–2.0 eV, when the delay time proceeds from –10 to 700 ps. At the late stage of 2  $\mu\text{s}$ , the induced spectral change almost disappears (see the lowest spectrum). The enhanced absorption observed in 2.2–3.0 eV is ascribed to the induced  $J$ -gap absorption. This indicates that the photoexcited  $e_g$  carriers suppress the spin correlations  $\langle S_i S_{i+1} \rangle$ , or decrease the macroscopic magnetization  $M$ . The similar photoinduced effect indicating the decrease of  $M$  was observed for  $\text{La}_{0.6}\text{Sr}_{0.4}\text{MnO}_3$  in the ferromagnetic phase.

The photoinduced effect is found to be strongly temperature dependent and observable only in the spin-polarized ferromagnetic phase ( $\leq 155 \text{ K}$ ). As shown in Fig. 2, we see a large absorption increase, and the spectral change is almost independent of temperatures below 93 K ( $\ll T_c$ ) both in the regions of 2.2–3.0 eV and 1.6–2.0 eV. With further increasing temperatures beyond  $T_c$ , the spectral change of the interband transition (2.2–3.0 eV) becomes small. This observation is consistent with the above interpretation, that is, the photoexcited  $e_g$  carriers suppress the ferromagnetic spin cor-

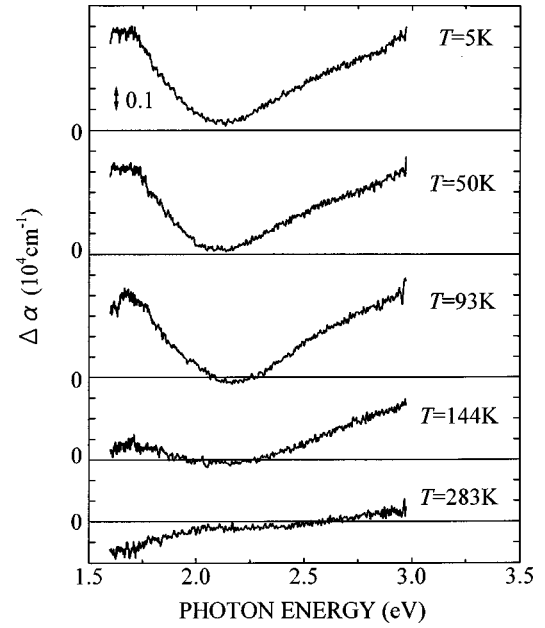


FIG. 2. Temperature dependence of the differential spectra measured at the delay time of 700 ps. The excitation photon energy and density are 3.20 eV and  $\sim 2 \times 10^{20} \text{ cm}^{-3}$ , respectively.

relation. The absorption decrease seen below 2.0 eV at  $T > T_c$  is not related to the  $J$ -gap transition, but associated with the small polaron transition. In the absorption spectrum above  $T_c$ , there exists a small polaron excitation band peaked at  $\sim 1.5 \text{ eV}$ .<sup>10</sup> As the optical transition between the small polaron and extended states is blocked under the pump-pulse-excitation condition, the absorption due to this transition is bleached. The induced absorption seen at  $T < T_c$  in the same energy region ( $< 2.0 \text{ eV}$ ) may be due to small polaron formation associated with the optical excitation of  $e_g$  carriers. A detailed study of small polarons is in progress.

As the spectral weight of the  $J$ -gap absorption band is proportional to  $[1 - (M/M_s)^2]$ , we can derive a magnetization change by pump-pulse excitation analyzing the spectral area of differential spectrum. The photoinduced change of spectral weight  $\Delta S = \int_{2.2 \text{ eV}}^{3.0 \text{ eV}} \Delta\alpha(\omega) d\omega$ , of the  $J$ -gap absorption is expressed by

$$\Delta S = C(M^2 - M'^2)/M_s^2, \quad (1)$$

where  $M$  and  $M'$  are magnetizations before and after pump-pulse excitations, respectively. The coefficient  $C$  is  $8.3 \times 10^3 \text{ eV cm}^{-1}$  for the spectral region studied here. Using Eq. (1), we obtain the photoinduced demagnetization  $\Delta M/M_s [= (M - M')/M_s]$  as large as 0.1 for the excitation density of  $\sim 8 \times 10^{19} \text{ cm}^{-3}$  with the photon energy of 3.20 eV at the delay time of 700 ps. Taking the Mn site density as  $2 \times 10^{22} \text{ cm}^{-3}$ , the demagnetization of  $0.1M_s$  means that one photoexcited  $e_g$  electron reverses the direction of about  $30t_{2g}$  spins.

The efficiency of the magnetization change is strongly dependent on the spin direction of the excited  $e_g$  electrons. The spin direction can be controlled with changing the excitation photon energy  $E_{ex}$ : the up- (down-) spin electrons are excited when  $E_{ex}$  is below (above)  $\sim 2.5 \text{ eV}$ . Figure 3 shows

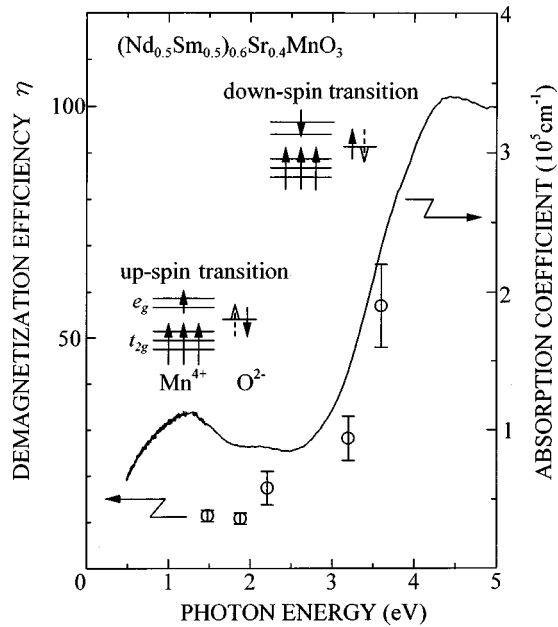


FIG. 3. Photon energy dependence of demagnetization efficiency (circle) together with the CT absorption spectrum [hatched region in the inset of Fig. 1(a)]. The pulse duration and the excitation photon density are 20 ns and  $0.7\text{--}2.0 \times 10^{20} \text{ cm}^{-3}$ , respectively.

the demagnetization efficiency vs the excitation photon energy at 12 K together with the CT absorption spectrum [hatched region in the inset of Fig. 1(a)]. We define the demagnetization efficiency  $\eta$  as  $(\Delta M/M_s)(N_{\text{Mn}}/N_{ph})$ , where  $N_{\text{Mn}}$  and  $N_{ph}$  are the densities (numbers/ $\text{cm}^{-3}$ ) of the Mn site and absorbed photon, respectively. The  $\eta$  value increases above  $\sim 2.5$  eV and is enhanced at the down-spin transition. In the down-spin transition,  $e_g$  electrons having a spin antiparallel to the  $t_{2g}$ -localized spin are generated, and these electrons reverse the direction of  $t_{2g}$  spins. On the contrary, when up-spin  $e_g$  electrons are generated by the up-spin transition, they do not contribute to the change of  $t_{2g}$ -localized spins. The remaining efficiency seen in the low-energy region may be explained by the existence of a broad tail of the down-spin transition band. Here, we discuss the thermal contribution to the increase of demagnetization efficiency. The  $\eta$  value for 3.6 eV is about six times larger than that for 1.9 eV, while the energy deposited into the sample increases by a factor of 1.9 for the corresponding photon energies. In addition, the measured temperature dependence of  $M$  around 12 K is very weak.<sup>5</sup> Therefore, the observed enhancement of the demagnetization efficiency at the down-spin transition is not ascribed to the temperature rise caused by the pump pulse. As discussed in the following paragraph, dynamical behaviors on the ps-ns time scale also confirm the purely electronic process of  $e_g$  carriers injected by the pump pulse.

In order to obtain deeper insight into the dynamical aspect of the photoinduced spin disorder, temporal behaviors of the spectral change were also investigated using a time-resolved spectroscopy. Figure 4(a) shows the time evolution of the spectral change monitored at 2.8 eV on the ps time scale. In the paramagnetic phase at 270 K,  $\Delta\alpha$  increases quickly ( $\sim 1$  ps) and remains constant at the late stage up to 400 ps. In the ferromagnetic phase at 5 K, by contrast, different tem-

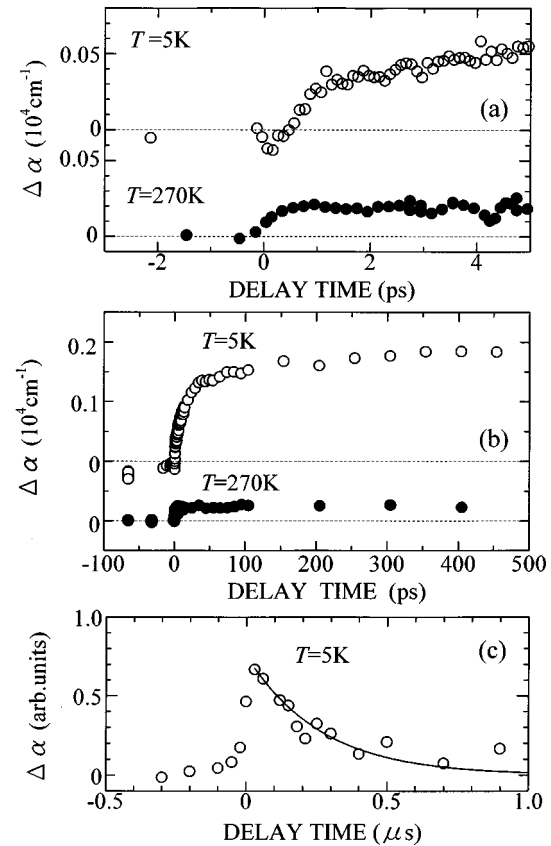


FIG. 4. (a) and (b) Time evolutions of absorption change  $\Delta\alpha$  measured at 2.8 eV for 5 and 270 K. The excitation photon energy and density are 3.20 eV and  $\sim 8 \times 10^{19} \text{ cm}^{-3}$ , respectively. (c) Time evolution of  $\Delta\alpha$  measured in the photon energy region of 2.0–3.0 eV on the  $\mu\text{s}$  time scale. The excitation photon energy and density are 3.20 eV and  $\sim 2 \times 10^{20} \text{ cm}^{-3}$ , respectively. The solid line represents the fitted curve assuming a single exponential decay with the decay time of 300 ns.

poral behaviors are observed, especially at the early stage of the delay time.  $\Delta\alpha$  decreases just after the pumping pulse, and increases within  $\sim 1$  ps. Although the bleaching component is small, the bleaching followed by the absorption increase is reproducible. The time scale of the negative  $\Delta\alpha$  (bleaching) is compared to the relaxation time (0.7 ps) of photoexcited carriers in the antiferromagnetic phase for prototypical CT insulators,  $\text{YBa}_2\text{Cu}_3\text{O}_{6.2}$  and  $\text{Nd}_2\text{CuO}_4$ .<sup>11</sup> This suggests that the fast bleaching component is ascribed to the nonradiative relaxation of photoexcited  $e_g$  carriers in the ferromagnetic phase. The upper panel of Fig. 4(b) shows the temporal behaviors of  $\Delta\alpha$  at the late stage. At 5 K,  $\Delta\alpha$  exhibits an initial rapid rise followed by a slow increase lasting about 200 ps, which is in contrast to the time-independent behavior between 5 and 400 ps observed at 270 K.

As the photoinduced demagnetization is sufficiently low ( $\Delta M/M_s \ll 1$ ),  $\Delta\alpha$  is approximately proportional to  $\Delta M$ . Thus, the relatively slow rise of  $\Delta\alpha$  reflects the characteristic behavior of  $\Delta M$  in the ferromagnetic phase. Defining a non-exponential rise time in which the signal increases from 10 to 90% of the maximum value, the rise time of the demagnetization is about 200 ps. The decay behavior on the  $\mu\text{s}$  time scale is shown in Fig. 4(c). The decay time of  $\Delta\alpha$  corresponding to the recovery time of the magnetization change is found to be about 300 ns. It is worthwhile to point out that

the slow rise time of  $\Delta\alpha$  observed at 5 K rules out the possibility of the lattice temperature rise caused by the pump pulse. As the lattice specific heat is larger at higher temperatures, the rise time of the absorption change due to the lattice temperature rise should be slower at 270 K.<sup>12</sup> In this experiment, however, the rise time at 270 K is as short as  $\sim 200$  fs.

We now propose the following scenario for the photoinduced demagnetization process. At the early stage after the photoexcitation ( $\leq 1$  ps), the photogenerated down-spin  $e_g$  electrons excite high-frequency spin waves of the  $t_{2g}$  spins ( $S=3/2$ ) via the strong on-site exchange interaction between the  $e_g$  spin and  $t_{2g}$  spin. Note that the up-spin  $e_g$  electrons scarcely excite the spin waves (see Fig. 3). The nonradiative relaxation of photoexcited  $e_g$  carriers occurs within  $\sim 1$  ps, whereas the excited spin waves induce a dynamical change of the  $t_{2g}$ -spin system up to  $\sim 300$  ns. The remaining spin waves continue to destroy the ferromagnetic spin ordering, and the disordered spin system may turn into an assembly of the ferromagnetic domains to reduce magnetostatic energies. Such a magnetic state may have a resemblance to the spin-glass state, since the excited magnetic system is quenched in a very short time ( $\leq 200$  ps). The spin-disordered state seems to be meta-stable, but finally collapses into the ferromagnetic ground state in 300 ns.

In summary, we have observed the significant spectral change by pump-pulse excitation in  $(\text{Nd}_{0.5}\text{Sm}_{0.5})_{1-x}\text{Sr}_x\text{MnO}_3$  ( $x=0.4$ ) thin film in the ferromagnetic phase. The increase of spectral weight is observed in the photon energy region of 2.2–3.0 eV, which indicates the photoinduced demagnetization of the localized Mn spin system. A demagnetization as large as  $0.1M_s$  takes place when the down-spin  $e_g$  carriers are injected by pump-pulse excitation ( $\sim 8 \times 10^{19} \text{ cm}^{-3}$ ). The time evolution of demagnetization has revealed a dynamical aspect of spin alignment in the double-exchange ferromagnet. The spin-disordered state is formed in 200 ps after the photoinjection of  $e_g$  carriers and the ferromagnetic ground state is recovered in 300 ns. The controllability of magnetization by the photoinjection of carriers indicates that the doped manganites have the potential for applications in magneto-optical devices with fast response times.

This work was partly supported by a Grant-in-Aid for Scientific Research from the Ministry of Education, Science, Sports and Culture of Japan. One of the authors (K.M.) acknowledges financial support by the Japan Society for the Promotion of Science for Japanese Junior Scientists.

\*Present address: Kanagawa Academy of Science and Technology, 3-2-1 Sakado, Takatsu-ku, Kawasaki, 213-0012, Japan.

<sup>1</sup>S. Koshihara, A. Oiwa, M. Hirasawa, S. Katsumoto, Y. Iye, C. Urano, H. Takagi, and H. Munekata, Phys. Rev. Lett. **78**, 4617 (1997).

<sup>2</sup>C. Buss, R. Pankoke, P. Leisching, J. Cibert, R. Frey, and C. Flytzanis, Phys. Rev. Lett. **78**, 4123 (1997).

<sup>3</sup>O. Sato, T. Iyoda, A. Fujishima, and K. Hashimoto, Science **272**, 704 (1996).

<sup>4</sup>P. W. Anderson and H. Hasegawa, Phys. Rev. **100**, 675 (1955).

<sup>5</sup>Y. Moritomo, A. Machida, K. Matsuda, and A. Nakamura, Phys. Rev. B **56**, 5088 (1997).

<sup>6</sup>Y. Okimoto, T. Katsufuji, T. Ishikawa, A. Urushibara, T. Arima, and Y. Tokura, Phys. Rev. Lett. **75**, 109 (1995).

<sup>7</sup>S. G. Kaplan, M. Quijada, H. D. Drew, D. B. Tanner, G. C. Xiong, R. Ramesh, C. Kwon, and T. Venkatesan, Phys. Rev. Lett. **77**, 2081 (1996).

<sup>8</sup>N. Furukawa, J. Phys. Soc. Jpn. **63**, 3214 (1994); **64**, 2734 (1995); **64**, 2754 (1995); **64**, 3164 (1995).

<sup>9</sup>K. Matsuda, M. Ichida, A. Nakamura, K. Kawamoto, T. Nabatame, and I. Hirabayashi, Physica C **280**, 84 (1997).

<sup>10</sup>A. Machida, Y. Moritomo, and A. Nakamura, Phys. Rev. B **58**, R4281 (1998).

<sup>11</sup>K. Matsuda, I. Hirabayashi, K. Kawamoto, T. Nabatame, T. Tokizaki, and A. Nakamura, Phys. Rev. B **50**, 4097 (1994).

<sup>12</sup>M. Mihailidi, Q. Xing, K. M. Yoo, and R. R. Alfano, Phys. Rev. B **49**, 3207 (1994).